

LEVERAGING NUMERICAL SIMULATIONS FOR MANAGING INSTALLATION RISKS

Paul Handidjaja*
Sterling Technical Services

Erick Kencana and Okky Purwana
Geo Oceanics

* Corresponding author: paul.handidjaja@sterlingtechnical.com

ABSTRACT

Leg penetration analysis serves as the primary basis for assessing jack-up installation risks. Among available techniques, analytical predictive methods are commonly used in routine assessments due to their practicality and generally reliable performance across many soil profiles. In complex stratified soil conditions, however, conventional analytical predictions may carry significant uncertainties. These uncertainties can hinder confident assessment of site suitability and the development of safe installation procedures. Moreover, relying on multiple independent predictions does not necessarily resolve these issues or strengthen stakeholder confidence in achieving a safe and successful installation.

This paper presents case histories of jack-up installations at four selected geotechnically challenging sites in Southeast Asia. Each site features complex soil profiles and presents unique challenges, including potentially insufficient leg length, severe leg runs, and multiple punch-through events. To support informed decision-making, the Coupled Eulerian-Lagrangian (CEL) approach within the Large Deformation Finite Element (LDFE) method was employed in the site assessments. Comparison among the analytical and numerical predictive framework against the actual spudcan penetration responses are highlighted.

KEY WORDS: jack-up, spudcan, penetration prediction, installation risks

1. INTRODUCTION

Large deformation finite element (LDFE) techniques for spudcan penetration simulations have been available in the past decade. The advancement of numerical modelling and computational power has made LDFE modelling become increasingly accessible to both researchers and practitioners. These developments have enabled more realistic modelling of spudcan penetration problems, including progressive failure mechanisms, soil plugging, and strain-softening responses that cannot be adequately captured by conventional analytical methods.

Despite its extensive use in research, the implementation of LDFE in practice remains limited. Its use has been largely confined to academic studies for benchmarking exercises of newly developed bearing capacity formula for two layers soil system. In routine practice, advanced modelling is sometimes viewed as introducing additional complexity and uncertainty into the assessment of installation risks, particularly when not explicitly justified by operational needs or project requirements. This perception has, in part, slowed the broader adoption of LDFE in routine jack-up installation risk mitigation practice.

Several studies on the benchmarking of numerical simulations of spudcan penetrations using LDFE approach against field data have been published. Hossain et al. (Ref. /1/) adopted LDFE using remeshing and interpolation technique with small strain (RITSS) technique to simulate spudcan penetrations in normally consolidated to lightly over-consolidated clay profiles for 14 case histories in the Gulf of Mexico. Hu et al. (Ref. /2/) and Hossain et al. (Ref. /3/) performed a series of LDFE analyses using CEL method to back simulate the spudcan punch through in sand overlying uniform clay based on case histories from numerous offshore sites. Mollaibrahimoglu et al (Ref. /4/) demonstrated the use of CEL modelling for validating existing analytical predictive methods for predicting punch-through resistance in multi-layered sand over clay profiles for various spudcan shapes.

There has been very limited information available in the public domain on the use of LDFE model for jack-up installations in complex stratified soil profiles and how the numerical approach can benefit risk identifications and associated mitigations in routine practice. This paper aims to share the experience of leveraging numerical simulations using CEL model to make informed decisions for jack-up deployments in challenging locations in the Southeast Asia region.

2. CASE STUDY

This paper highlights four installation sites, each presenting distinct geotechnical risks. Key site characteristics and the corresponding jack-up rigs are summarized in Table 1. At three sites, the soil conditions are predominantly clay, while one site is characterized by a layered profile of silty sand and clay. Three jack-up designs were deployed across the sites, with comparable spudcan bearing pressures ranging from 411 kPa to 461 kPa under maximum preload footing reaction. The soil conditions and predicted leg penetration behaviors are discussed in the following sections.

2.1 Soil Conditions

The undrained shear strength profiles inferred from the CPT boreholes at the installation sites are presented in Figure 1.

Site A is generally a thick deposit normally consolidated to lightly over consolidated clay up to 50 m depth below seabed and pose the risk of deep leg penetration and potentially leading to leg length restrictions. A stiff clay crust is present at approximately 25 m depth below seabed at the installation site leading to rapid leg penetration risk. Site B soil condition consists of multi-layered clays with multiple crusts varying from firm to very stiff clay. The complex soil stratigraphy results in high risk of punch-through at several depths. At Site C, the soil stratigraphy essentially comprises alternating silty sand and clay stratum. This leads to uncertainty as to whether punch through risk is present or spudcan is likely to hang up at shallow penetration. Site D has similar characteristics to Site B.

2.2 Predicted Leg Penetration Behaviour

Spudcan penetration analysis was initially performed using ISO 19905-1 (Ref. /5/) method assuming full backfill condition. The predicted load-penetration curves are presented in Figure 3 to 6 for Site A to D respectively. Particularly for Site C, sand plug was not considered. The geotechnical risks identified from the analytical spudcan penetration predictions at all the four sites include deep penetration and the associated restricted leg length, punch-through at high preload level, severe leg run, and leg hang up at full preload leaving an uncertainty in the bearing capacity margin beyond applied preload.

At Site A, the final spudcan tip penetration depth under the maximum preload footing reaction was estimated to be between 27.5 m and 32.2 m. There was a risk of rapid leg penetration from 20.0 to 25.0 m corresponding to 67% and 87% preload. Moderate rate of leg penetration was expected for depths greater than 25 m. If the lower bound soil shear strength profile was realized, the leg reserve at the maximum preload was estimated to be marginal at only 5 m.

At Site B, the anticipated final penetration depth spanned a wide range of 15.8 m to 34.1 m under maximum preload. While leg reserve was sufficient, two major concerns were noted: (i) the risk of punch-through at high preload levels, and (ii) uncertain soil resistance margins in the event of leg hang-up at full preload. The risk of punch-through was expected to be between 77% and 100% preload. If the soil shear strength followed the inferred lower bound, the predicted penetration would exceed the maximum allowable depth specified in the unit's operations manual.

At Site C, a wide range of potential penetration depths were predicted, from a shallow 4.4 m hang-up to as deep as 25.0 m. The risks included a punch-through at high preload levels and leg hang-up at full preload with little or no reserve margin. Severe leg run from 4.4 m to 25.0 m depth was anticipated between 75 and 100% preload. Conversely, if the upper-bound soil strength profile were realized, the leg would likely hang up with minimal margin beyond full preload.

At Site D, punch-through risk was identified when preload level is between 72 and 90%. The spudcan tip was expected to reach a relatively narrow penetration range of 13.4 m to 15.8 m at maximum preload.

Table 1 Summary of Site Characteristics

Site	A	B	C	D
Soil condition	Generally, NC to lightly OC clay	Multi-layered clays	Multi-layered silty sand-clay	Multi-layered clays
Identified installation risks	Deep penetration, Rapid leg penetration, Restricted leg length	Deep penetration, Punch-through at high preload level, leg hang-up at full preload	Punch-through at high preload level, severe leg run, leg hang-up at full preload,	Punch-through at high preload reaction
Water depth (m LAT)	97.6	60.3	55.2	62.0
Total leg length (m)	169.0	157.6	133.2	157.6
UB/LB spudcan tip depth – ISO 19905-1 (m)	27.5/32.2	15.8/34.1	4.4/25.0	13.4/15.8
Airgap – LAT to keel (m)	15.7	12.5	12.5	12.5
Fixed height (m)	18.5	15.8	15.8	15.8
Leg reserve (m)	5.0	35.7	49.1	51.4
Spudcan diameter (m)	18.3	15.2	14.0	15.2
Bearing pressure at maximum preload reaction (kPa)	446	411	461	411

Based on the initial assessment, jack-up installations at these locations were considered high risk, leading to significant uncertainties in informed decision-making. To strengthen stakeholder confidence and support the final decision, additional data was required to benchmark the initial predictions. Subsequently, LDFE simulations using the CEL method were performed to address the inherent limitations of analytical solutions and to model spudcan penetrations in a more realistic manner.

3. NUMERICAL MODELLING

3.1 General Strategy

To optimize the numerical simulations, generally the weakest soil profile was first selected based on the load penetration responses predicted using the analytical solution. Design lower bound soil shear strength of the selected soil profile was adopted. This allows identification of the deepest possible penetration and the earliest onset of punch-through. The latter is useful for checking the feasibility of minimum preload footing reaction to avoid punch-through risk and deep penetration. This provides reference to developing preloading strategies, starting with the weakest location.

3.2 Soil Constitutive Models

The strain-softening Tresca model proposed by Einav & Randolph (Ref. /6/) is adopted for clay to simulate strength degradation mechanisms commonly encountered in clay undergoing large deformations. The Tresca model is a sub-class of the conventional Mohr-coulomb model with zero friction angle and zero dilatancy angle and is often used in total stress analysis to simulate soil failure conditions. To simulate clay soil exhibiting strain-softening behavior, the conventional Tresca model is further modified by reducing its yield surface size to capture the strain-softening behavior. Non-associated flow rule-based Mohr-Coulomb model is adopted for sand allowing non-zero internal friction angle and zero dilatation angle.

Through advection process, soil can flow within the fixed mesh configurations. The soil material is tracked concurrently with the soil flow ensuring realistic evolution of soil movement around a penetrating spudcan. This is especially important for realistic simulation of a spudcan penetrating multiple subsurface layers (Ref. /7/).

3.3 Numerical Modelling

The CEL simulation was performed in Abaqus. The horizontal boundary of the soil domain was fixed at 2.75 times the spudcan width measured from the spudcan edge. This clearance is deemed to be sufficiently large to minimise the boundary effects while allowing an optimum computational time. The bottom boundary of the soil domain is set at a depth of 30-50 m from the mudline representing the bottom strong soil layer. A fine mesh size, approximately 0.025 times the spudcan width, is used within 0.75 times the spudcan diameter from the symmetry axis to cover significant soil movements induced by the spudcan penetration. For saving computation time and taking advantage of the symmetrical shape of the spudcan, only half of the domain is included in the model. Zero flow velocity was prescribed normal to this plane of symmetry.

The soil domain consists of 8-noded Eulerian brick elements denoted as EC3D8R of approximately 950,000 in size. A void layer was defined above the mudline to allow the soil to heave. The undrained shear strength was allowed to reduce to its remolding state due to strain softening behavior depending on the accumulated plastic shear strain. The clay sensitivity was determined according to the respective laboratory shear strength tests data for each site. A ratio of E_u/s_u of 150 is assumed for the clay layer while the Poisson's ratio is set to be 0.30 and 0.495 for sand and clay respectively. An example of the finite element mesh is shown in Figure 2.

For enhanced computational efficiency, the spudcan was modelled as a rigid shell part instead of using solid deformable brick elements which is computationally more time consuming. The spudcan was modelled with approximately 3,000 discrete rigid Lagrangian R3D4 elements. The interface between the spudcan and soil was modelled using surface-to-surface contact formulation to formulate the normal and tangential behaviours. The hard contact pressure-overclosure relationship was adopted for the normal behaviour with zero-penetration conditions but allowed separation after contact. The basic isotropic Coulomb friction model is adopted for the tangential behaviour formulated based on the penalty method.

In order to achieve a balance between matching a quasi-static state as closely as possible and at the same time reducing the computational time, the spudcan was set to continuously penetrate into the seabed through the application of a prescribed velocity of 0.2 m/s. At this rate of spudcan penetration, the inertial effect is deemed to be negligible.

3.4 Numerical Simulations Results

The numerical simulation results are superimposed with the analytical predictions in Figure 3 to Figure 6. In addition, post-installation soil shear strength profiles and plastic strains contours at the predicted final penetration depth corresponding to each numerically derived load-penetration response are also presented.

At Site A, the overall trend of the load-penetration response aligns with the analytical prediction. For the same lower bound shear strength profile, the CEL simulation produces a higher soil resistance at a given depth. This can be attributed to the CEL model's ability to capture the influence zone beneath the spudcan which enhances penetration resistance for the design soil profile.

Punch-through risk at the first peak identified at Site B does not appear in the CEL result. Instead, gradual spudcan penetrations are observed which can be attributed to temporary clay-plugging as the spudcan pushes through the top stiff clay. The second peak occurs at a fairly higher soil resistance than the full preload reaction and followed by a more "ductile" post-peak response compared to the analytical prediction. Under the lower bound soil shear strength, spudcan hang-up is predicted at the full preload. This is contrary to the corresponding analytical prediction which suggests a severe punch-through and leg run to 34.1m depth during preloading.

As opposed to punch-through risk, at Site C the CEL simulation exhibits squeezing mechanism as the spudcan penetrates the top sand layer. The peak resistance occurs at a significantly larger footing reaction than the analytical prediction with the lower bound soil shear strength. The spudcan is expected to hang up at the full preload level. Beyond this, the spudcan undergoes a rapid penetration equal to the thickness of the underlying layer.

The first and second peaks predicted analytically for Site D do not appear in the CEL simulation. Instead, the spudcan advances gradually from 2m to 16m tip depth before reaching the very stiff clay layer.

4. ACTUAL SPUDCAN PENETRATION RESPONSES

A preloading strategy was put in place to mitigate the identified punch-through risk. The preloading operation was carried out in two stages with the hull in water at 1 m draft. A complete cycle of sequential leg preloading was first completed at a partial preload level followed by a second cycle to achieve the full preload target. Hull jacking was made periodically to maintain level conditions and return the hull to the initial draft. At several sites, a reduced preload determined through site-specific assessment was applied to further minimize installation risks.

The actual spudcan penetration responses at the four installation sites are summarized in Table 2. In the following section, the actual spudcan penetration responses at each installation site and their comparison against both analytical and numerical predictions are described in detail. It is important to note that the CEL simulations were performed using the lower bound soil shear strength profile whereas the actual penetrations should correspond to the best estimate soil profile. This assumes the prediction methods can realistically capture the progressive bearing capacity failure mechanism during spudcan penetration.

Table 2 Summary of Actual Spudcan Penetration Response

Site	A	B	C	D
Soil condition	Generally NC to lightly OC clay	Multi-layered clays	Multi-layered silty sand-clay	Multi-layered clays
Actual spudcan penetration response	Controlled minor rapid leg penetration, final penetration depth within anticipated range	Controlled gradual penetration	Minor settlement during preloading, spudcan hang-up at full preload	Controlled gradual penetration
Analytical prediction -UB/LB (m)	27.5/32.2	15.8/34.1	4.4/25.0	13.4/15.8
Numerical prediction - LB (m)	27.6	15.5	4.7	15.3
Actual spudcan tip depth (m)	27.6	14.2	4.2	14.4

The actual spudcan penetration trajectory is generally consistent with the numerical simulation for Site A. The final spudcan tip penetration depth is well predicted by the CEL model and coincides with the analytical prediction based on the upper bound soil shear strength profile. This suggests that the CEL model can serve the intended purpose for providing reliable estimates of the maximum possible spudcan penetration and leg length utilization with greater confidence.

At Site B, the CEL simulation confirms that the punch-through risk at the first peak is less severe than suggested by the analytical prediction. The actual post-peak spudcan penetration response is gradual which agrees closely with the numerical simulation. Although the final penetration depth is somewhat shallower than predicted, the observed trajectory demonstrates that the second peak from the lower bound analytical prediction is overly conservative. In this regard, the CEL result provides assurance that adequate soil resistance exists beyond the preloaded level.

At the Site C, the spudcan experienced minimal settlement during preloading and remained hung up at the final preload level. Similar to Site B, CEL result shows that the analytical prediction is overly

conservative in this case and that additional bearing capacity beyond the preloaded level is available.

The actual spudcan penetration behavior at the Site D validates the gradual penetration response predicted by the CEL simulation is realistic. A minor leg run was recorded but the final penetration depth is in good agreement with the numerical prediction. The observed penetration trajectory however more closely follows the lower bound soil shear strength profile which may be influenced by the selection of cone factor.

5. SUMMARY

This study highlights the value of numerical simulations as a complementary tool to analytical methods for predicting spudcan penetration in complex soil conditions. Where installation risks are identified as severe and uncertainty is high, numerical simulations can provide critical additional input for informed decision-making. While all prediction methods involve some degree of uncertainty, numerical simulations can capture the underlying soil resistance mechanisms more realistically than analytical approaches and, in some cases, reduce the perceived severity of installation risks.

In the limited case studies presented, the use of CEL simulations has demonstrated clear benefits by offering deeper insights into potential installation challenges and enhancing confidence level in the installation procedures. As more benchmarking studies become available, the reliability of CEL modelling can be progressively improved, ultimately providing greater assurance for the safe installation of jack-up rigs in challenging locations.

6. ACKNOWLEDGEMENTS

The authors acknowledge the support from PetroVietnam Drilling team for their permission to publish this technical paper.

7. REFERENCES

- [1] Hossain, M.S., Zheng, J., Menzies, D., Meyer, L., Randolph, M.F. (2004). Spudcan Penetration Analysis for Case Histories in Clay, *Journal of Geotechnical & Geoenvironmental. Engineering*, 2014: 140(7).
- [2] Hu, P., Haghighi, A., Coronado, J., Leo, C., Liyanapathirana, S. and Li, Z. (2021). A comparison of jack-up spudcan penetration predictions and recorded field data, *Applied Ocean Research* 112.
- [3] Hossain, M.S., Hu, P., Cassidy, M.J., Menzies, D. and Winsgate, A. (2019). Measured and calculated spudcan penetration profiles for case histories in sand-over-clay, *Applied Ocean Research* 82 (2019): 447–457.
- [4] Mollaibrahimoglu, C., Sharp, L., van Tongeren, A., Hill, A.R. and Purwana, O.A. (2023). “Improving Performance of Spudcan Predictions during Installation”, *Jack-up Conference*, City University, London.
- [5] ISO 19905-1. (2016). Petroleum and natural gas industries — Site-specific assessment of mobile offshore units —Part 1: Jack-ups, 2016.
- [6] Einav, I. and Randolph, M. F. (2005). “Combining upper bound and strain path methods for evaluating penetration resistance”. *Int. J. Numer. Methods Engng* 63, No. 14, 1991–2016.
- [7] Tho, K.K., Leung, C.F., Chow, Y.K. and Swaddiwudhipong, S. (2011). “Important Considerations in the Application of Eulerian Technique for Spudcan Penetration Analysis”. *13th Jack-up Conference*, City University, London.

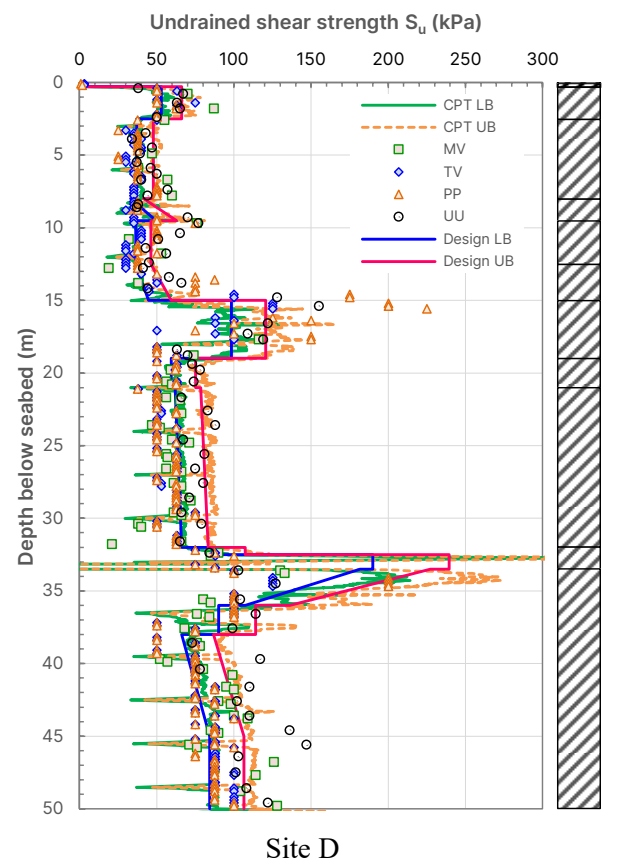
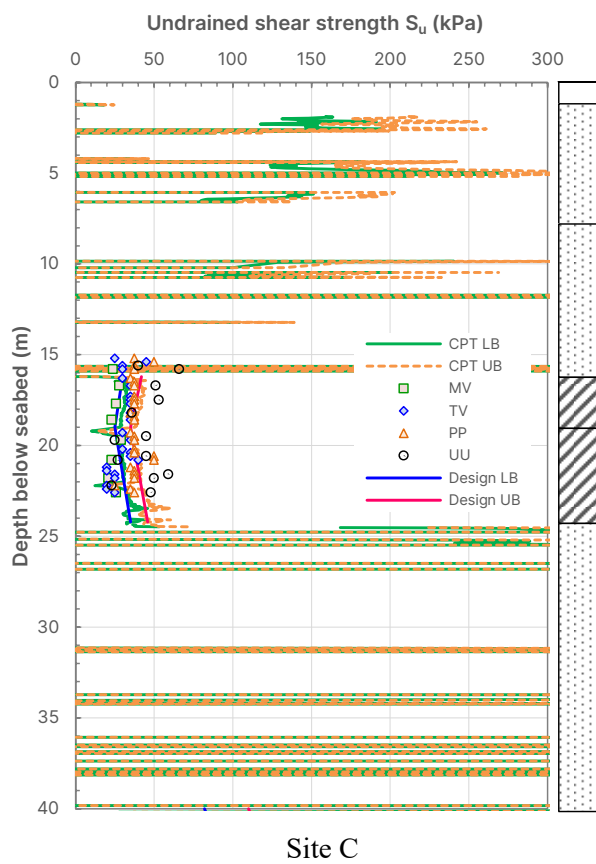
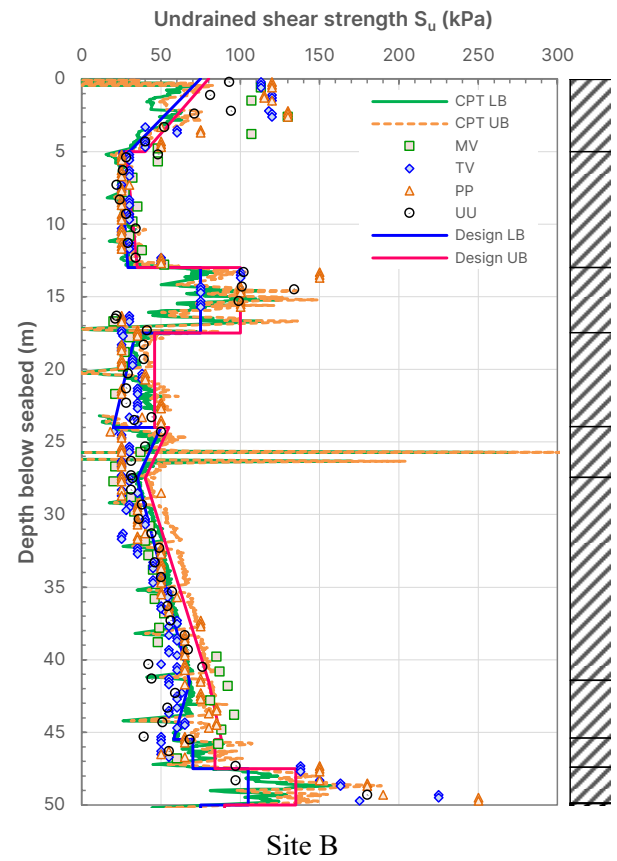
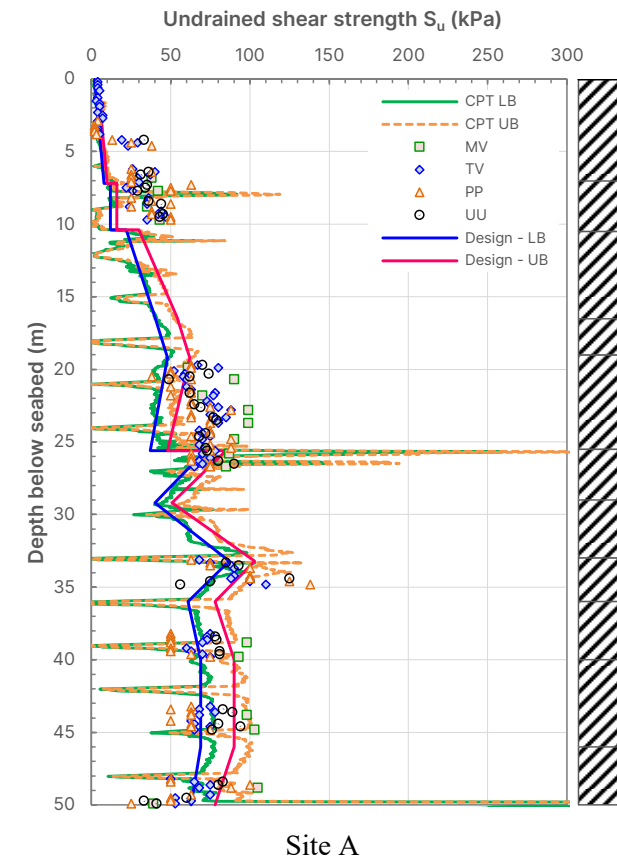


Figure 1 Design soil profiles

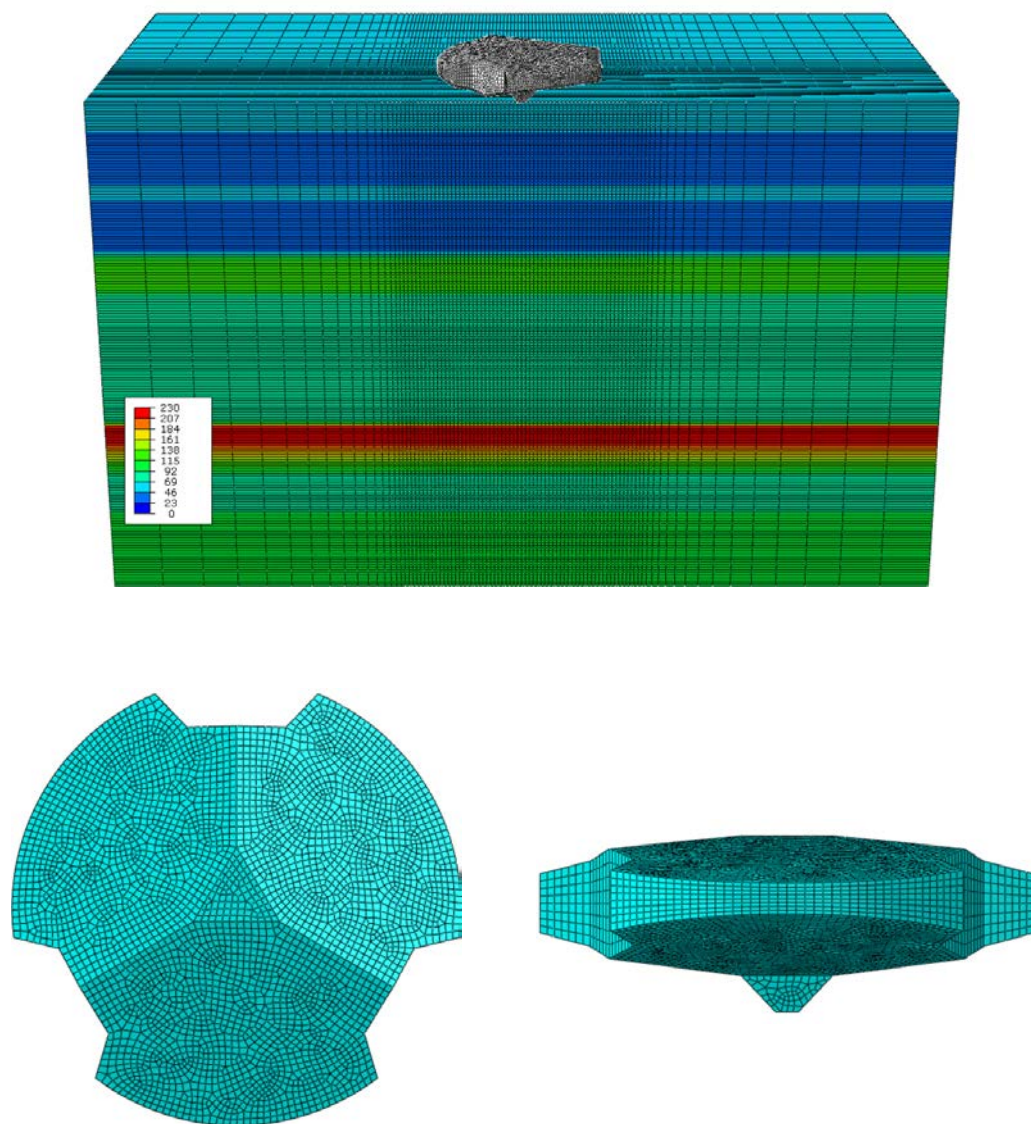


Figure 2 Example finite element model of soil domain and spudcan

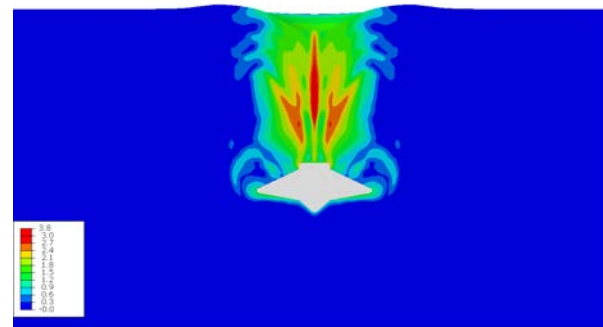
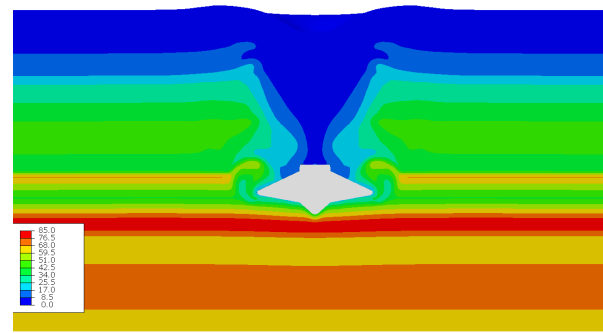
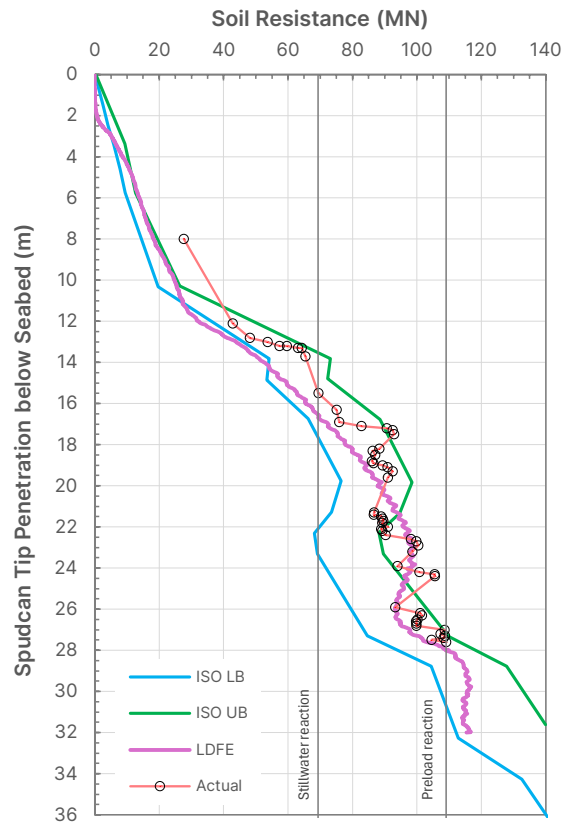


Figure 3 Spudcan penetration response and soil failure mechanism (SITE A)

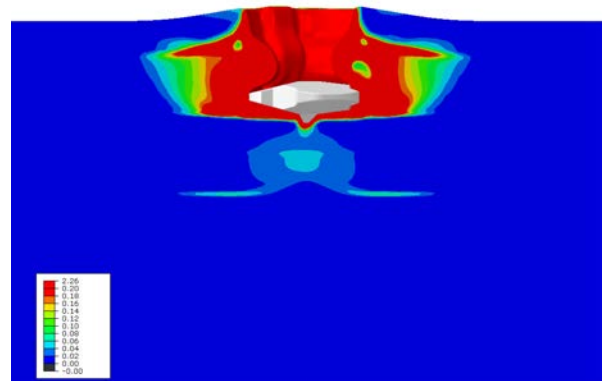
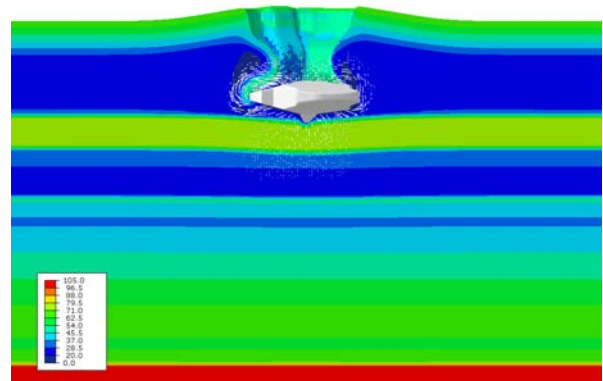
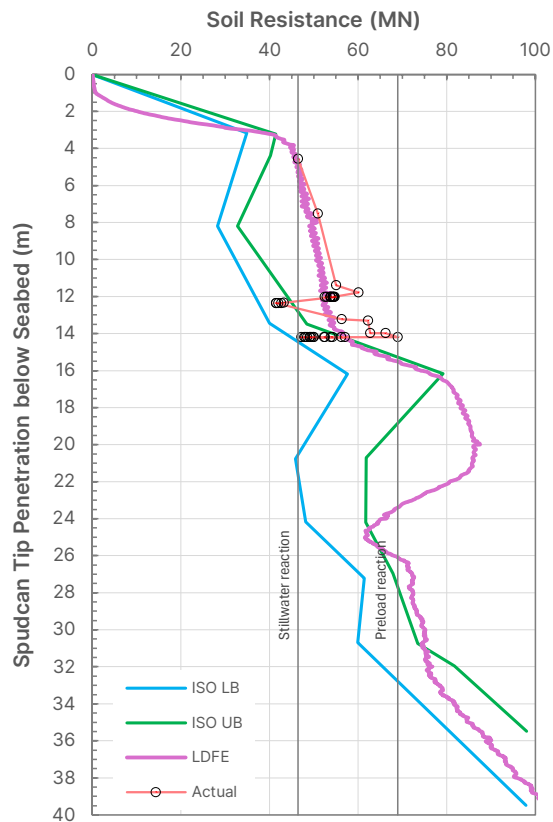
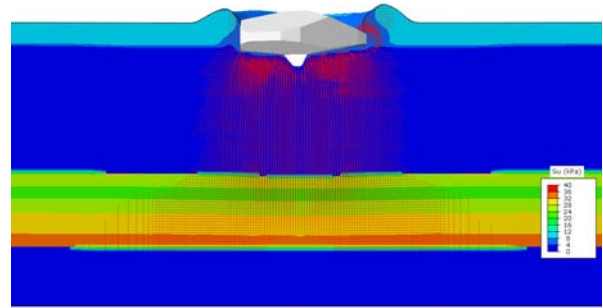
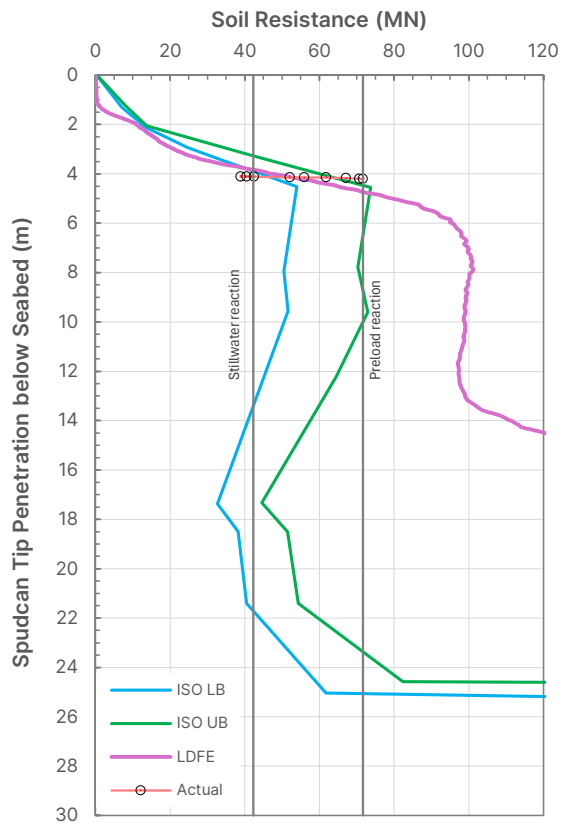
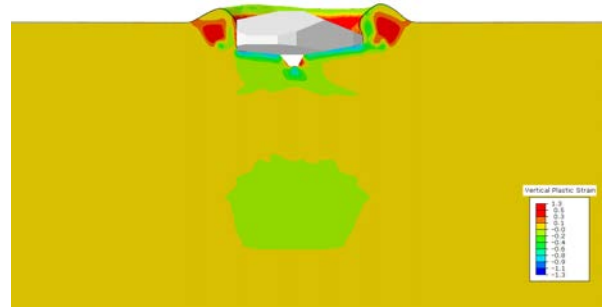


Figure 4 Spudcan penetration response and soil failure mechanism (SITE B)

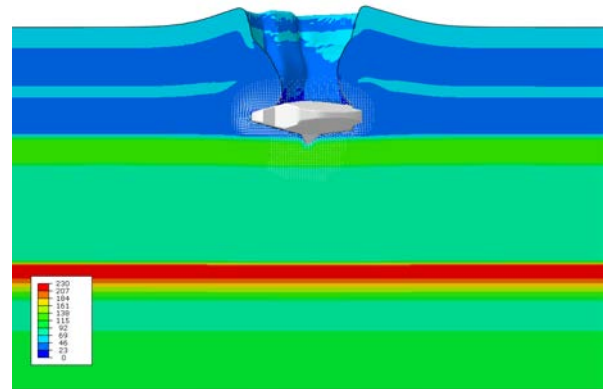
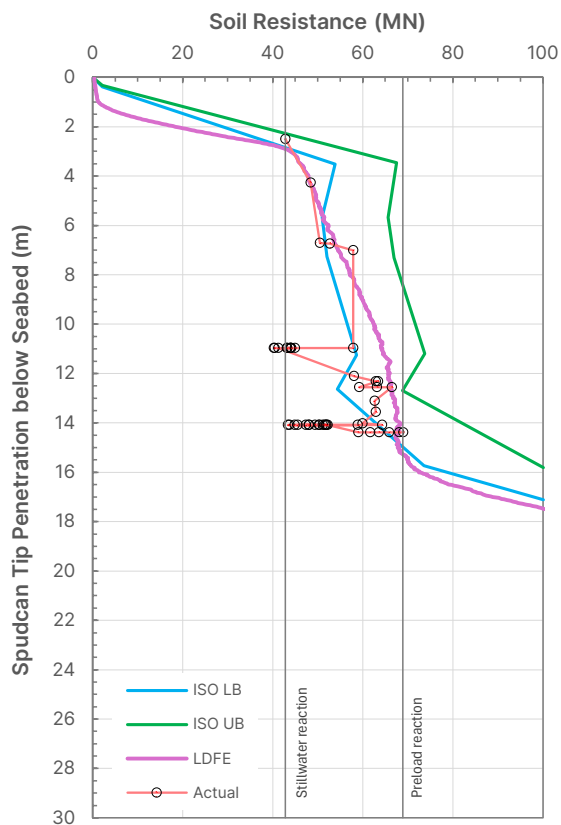


Change in soil shear strength profile

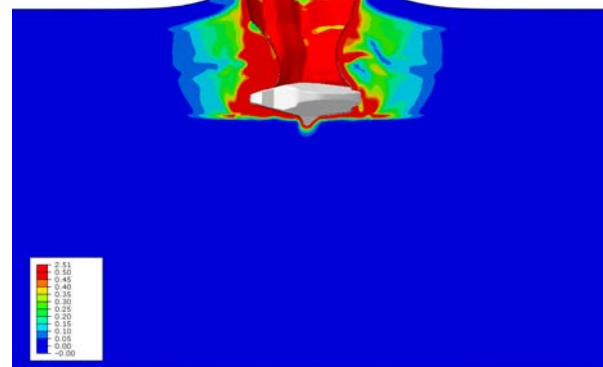


Plastic strain at final penetration depth

Figure 5 Spudcan penetration response and soil failure mechanism (SITE C)



Change in soil shear strength profile



Plastic strain at final penetration depth

Figure 6 Spudcan penetration response and soil failure mechanism (SITE D)